Effect of the Lipid Phase Transition on the Lactose Permease from *Escherichia coli*†

Wei Zhang and H. Ronald Kaback*

Howard Hughes Medical Institute, Departments of Physiology and Microbiology & Molecular Genetics, Molecular Biology Institute, University of California Los Angeles, Los Angeles, California 90095-1662

Received August 16, 2000; Revised Manuscript Received September 21, 2000

ABSTRACT: The temperature dependence of lactose active transport, efflux down a concentration gradient, and equilibrium exchange were analyzed in right-side-out membrane vesicles from *Escherichia coli* containing wild-type lactose permease and mutant Glu325 → Ala. With respect to uphill transport and efflux down a concentration gradient, both of which involve H^+ symport, Arrhenius plots with wild-type permease exhibit a discontinuity at 18−19 °C with a 7−8-fold decrease in activation energy above the phase transition. For equilibrium exchange, which does not involve H^+ symport, the change in activation energy is much less pronounced (2−3-fold) than that observed for active transport or efflux. Strikingly, mutant Glu325 → Ala, which catalyzes equilibrium exchange as well as wild-type permease but is defective in all translocation reactions that involve net H^+ translocation, exhibits no change whatsoever in activation energy. The findings are consistent with the conclusion that the primary effect of the lipid phase transition is to alter coupling between substrate and H^+ translocation rather than the conformational change(s) responsible for translocation across the membrane.

Temperature-induced phase transitions of phospholipids in biological membranes have been used to study structure−function relationships between membrane proteins and their lipid environment. The thermal phase transition is detected by methods that include X-ray diffraction (*1*), microcalorimetry (*2*), or fluorescence spectroscopy (*3*) and is attributed to conversion of the fatty acyl side chains of the membrane phospholipids from an ordered, gel-like state below the phase transition to a disordered, more liquid-like state above the phase transition (*4*). The temperature at which the transition occurs is dependent primarily upon the properties of the fatty acyl side chains of the membrane phospholipids (*5*−*7*), and the influence of the lipid phase transition on the function of membrane proteins is generally studied by measuring activity as a function of temperature and determining activation energy (E_a) by using Arrhenius analysis (see ref *8*). For the great majority of soluble enzymes, Arrhenius plots are linear over a wide temperature range. For membrane-embedded enzymes, however, nonlinear plots with an abrupt change in activation energy corresponding to the lipid phase transition are frequently observed (*7*, *9*, *10*). More specifically, active transport by lactose permease (lac permease)[1] of *Escherichia coli* exhibits a sharp discontinuity at 18−19 °C that correlates with the lipid phase transition (*6*, *11*, *12*), and it has been postulated that the phase transition exerts its primary effect on the translocation of the ternary complex between the permease, substrate, and H^+ across the membrane (see ref *8*).

The lac permease is a paradigm for secondary transport proteins that couple free energy stored in an electrochemical ion gradient into a substrate concentration gradient (*13*−*16*). This hydrophobic, polytopic membrane protein catalyzes the coupled stoichiometric translocation of galactosides and H^+, and the permease has been solubilized, purified to homogeneity, reconstituted into proteoliposomes, and shown to be solely responsible for galactoside transport (reviewed in ref *17*) as a monomer (see ref *18*). The permease is composed of 12 α-helices that traverse the membrane in zigzag fashion connected by hydrophilic loops with the N and C termini on the cytoplasmic face (Figure 1) (*19*, *20*). Moreover, a model describing helix packing has been constructed by means of extensive site-directed mutagenesis combined with a battery of site-directed biochemical and biophysical techniques (*21*).

Site-directed mutagenesis of wild-type permease and Cys-scanning mutagenesis of a functional mutant devoid of Cys residues reveal that only six residues in the permease are irreplaceable with respect to active transport and/or ligand binding: Glu126 (helix IV) and Arg144 (helix V) are critically involved in substrate binding, and Glu269 (helix VIII), Arg302 (helix IX), His322, and Glu325 (helix X) play essential roles in H^+ translocation and coupling (reviewed in ref *22*). The overall mechanism for lactose/H^+ symport involves a minimum of six kinetic steps (Figure 2): (i) binding of H^+ to the permease; (ii) binding of substrate; (iii) translocation of the ternary complex across the membrane; (iv) release of substrate; (v) release of H^+; and (vi) return of the unloaded permease to the opposite surface. In contrast, exchange and counterflow involve steps 2 to 4, which do not involve H^+ translocation (*23*, *24*). In addition to active transport, lactose efflux, exchange, and counterflow are

†This work was supported in part by NIH Grant DK51131 to H.R.K.

* To whom correspondence should be addressed. E-mail: RonaldK@HHMI.UCLA.edu.

[1] Abbreviations: lac permease, lactose permease; RSO, right-side-out; KP_i, potassium phosphate; PMS, phenazine methosulfate.

10.1021/bi001947g CCC: $19.00
Published on Web 11/03/2000

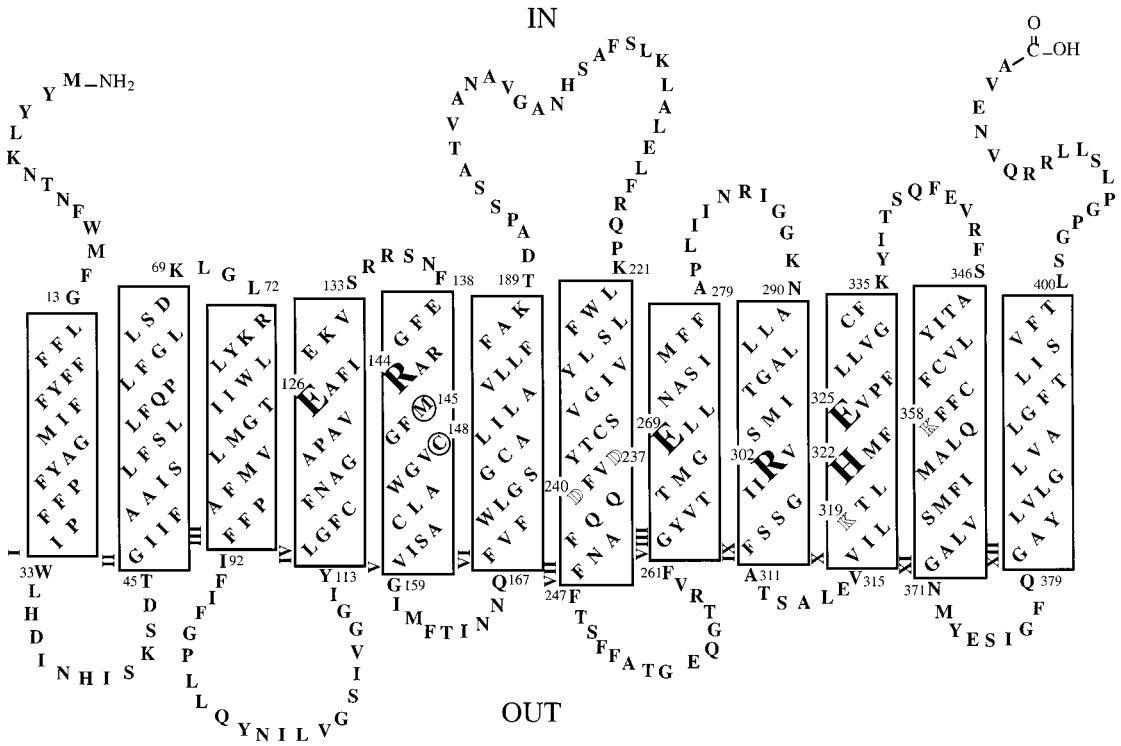

FIGURE 1: Secondary structure model of lac permease. The single-letter amino acid code is used, and transmembrane helices are shown in boxes. The positions of the six irreplaceable residues Glu126, Arg144, Glu269, Arg302, His322, and Glu325 are emboldened. Charge pairs Asp237/Lys358 and Asp240/Lys319 are shown in outline. Cys148 which interacts hydrophobically with the β-face of the galactosyl moiety of substrate and Met145 which interacts with the anomeric substituent of certain substrates are encircled.

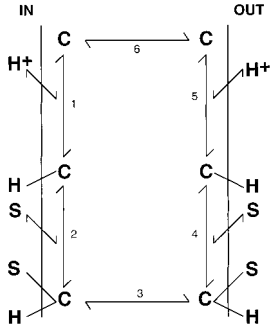

FIGURE 2: Schematic representation of reactions involved in lactose/H^+ symport. C represents lac permease; S is substrate (lactose).

blocked in His322, Arg302, and Glu269 mutants. However, permease mutants with neutral replacements for Glu325 are defective in all steps that involve net H^+ translocation, but bind ligand and catalyze exchange and counterflow as well or even better than wild-type permease (*25*−*27*).

In this communication, the effect of the lipid phase transition on the various translocation reactions catalyzed by lac permease is examined. Evidence is presented demonstrating that the abrupt change in activation energy observed at the phase transition is due to an effect on coupling between substrate and H^+ translocation rather than an effect on translocation across the membrane.

EXPERIMENTAL PROCEDURES

Growth of Bacteria. E. coli T184 [lacI$^+$O$^+$Z$^-$Y$^-$ (A), *rspL*, *met*, *thr*, *recA*, *hsdM*, *hsdR/F′*, lacI^{q}O$^+$Z^{u118}(Y$^+$A$^+$)] (*28*) expressing wild-type lac permease or E325A,[2] E325D mutants were grown acrobically at 37 °C overnight in Luria−Bertani medium containing ampicillin (100 μg/mL). Fully grown cultures were diluted 10-fold and allowed to grow for 2 h at 37 °C before induction with 1.0 mM *i*-propyl 1-thio-β-D-galactopyranoside (final concentration). After further growth for 2 h at 37 °C, cells were harvested by centrifugation and used for preparation of right-side-out (RSO) membrane vesicles.

Preparation of RSO Membrane Vesicles. RSO membrane vesicles were prepared by lysozyme-ethylenediaminetetraacetate treatment and osmotic lysis (*29*, *30*). The vesicles were suspended at a protein concentration of 10−15 mg/mL in 100 mM potassium phosphate (KP_I; pH 7.5)/10 mM $MgSO_4$, frozen in liquid N_2 and stored at −80 °C until use.

Transport Assays. For active transport, RSO membrane vesicles were washed once with 100 mM KP_i (pH 7.5)/10 mM $MgSO_4$ and resuspended to a protein concentration of 4.0 mg/mL. Initial rates of active transport of [1-^{14}C]lactose (2.5 mCi/mmol; final concentration of 0.4 mM) were measured as a function of temperature in the presence of 20 mM potassium ascorbate and 0.2 mM phenazine methosulfate (PMS) under oxygen (*31*). Briefly, aliquots of the vesicle suspension (50 μL) were incubated at a given temperature for 15 min under oxygen prior to addition of potassium ascorbate, PMS, and [1-^{14}C]lactose. Reactions were quenched at given times with 100 mM KP_i (pH 5.5)/100 mM lithium chloride and assayed by rapid filtration (*32*). Rates were estimated from the initial linear phase of the time courses. The data presented represent the average of at least four independent experiments; the error bars represent the standard error of the mean (SEM).

[2] Site-directed mutants are designated by the single-letter amino acid abbreviation for the targeted residue, followed by the sequence position of the residue in the wild-type permease, followed by a second letter indicating the amino acid replacement.

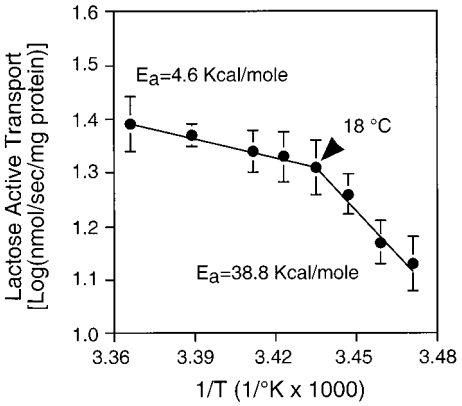

FIGURE 3: Arrhenius plot of active lactose transport by RSO membrane vesicles containing wild-type permease. Measurements were carried out under oxygen in the presence of potassium ascorbate and PMS with [1-^{14}C]lactose at a final concentration of 0.4 mM as described in Experimental Procedures. Initial rates of transport were estimated from the initial linear phase (i.e., within 20 s). The results shown are the average of at least four independent experiments, and the bars represent the SEM. E_a values were calculated from the slopes shown by using the Arrhenius equation (see ref *8*). The arrowhead depicts the temperature at which the discontinuity occurs.

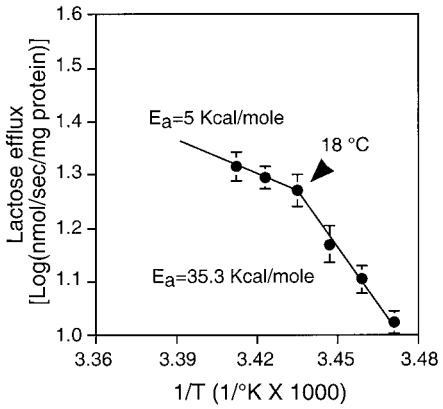

FIGURE 4: Arrhenius plot of lactose efflux by RSO membrane vesicles containing wild-type permease. RSO vesicles were equilibrated with 10 mM [1-^{14}C]lactose and assayed by dilution into equilibration buffer without lactose at given temperatures, as described in Experimental Procedures. Initial rates of [1-^{14}C]lactose efflux were estimated from the initial linear phase of transport (i.e., within 20 s). The results shown are the average of at least four independent experiments, and the bars represent the SEM. E_a values were calculated from the slopes shown by using the Arrhenius equation (see ref *8*). The arrowhead depicts the temperature at which the discontinuity occurs.

Efflux and equilibrium exchange were performed as described (*24*). For each type of assay, vesicle suspensions and diluents were equilibrated at given temperature in a thermal cycler for 15 min, and assays were carried out at the same temperature. RSO membrane vesicles were washed with 100 mM KP_i (pH 7.5)/10 mM $MgSO_4$ and resuspended to a protein concentration of 30 mg/mL, and valinomycin and nigericin were added at final concentrations of 20 and 0.2 μM, respectively. [1-^{14}C]Lactose (10 mCi/mmol) was added to a final concentration of 10 mM, and the samples were incubated at 4 °C overnight. Aliquots (2.0 μL) of pre-equilibrated vesicles were then rapidly diluted 200-fold into 0.4 mL of 100 mM KP_i (pH 7.5) alone (efflux) or containing 10 mM unlabeled lactose (equilibrium exchange). Reactions were quenched at given times with 100 mM KP_i (pH 5.5)/100 mM lithium chloride and assayed by rapid filtration. Rates were estimated from the initial linear phase of the time courses.

Data Analysis. Initial rates of transport estimated from the linear phase of influx or efflux under the conditions described was assayed at temperatures ranging from 10 to 25 °C, and the data were analyzed according to Arrhenius where activation energy in kilocalories/mol (kcal/mol) is determined from the slope of the function obtained by plotting the log of the initial rate versus temperature^{-1} (see ref *8*).

RESULTS

Active Transport. As demonstrated previously with intact cells (*7*, *9*) as well as RSO membrane vesicles (*11*), respiration-driven active lactose transport catalyzed by lac permease exhibits a nonlinear Arrhenius plot between 13 and 25 °C with an abrupt discontinuity at 18−19 °C that corresponds to the thermal phase transition of the phospholipids in wild-type *E. coli* membranes (Figure 3). The activation energy (E_a) at temperatures below the phase transition is calculated to be about 38.8 kcal/mol (163 kJ/mol), while above the phase transition, E_a, is about 4.6 kcal/mol (19.3 kJ/mol). Thus, the ratio of E_a values below and above the phase transition approximates 8.4. Although data are not presented, the proton electrochemical gradient ($\Delta\bar{\mu}_{H^+}$), as measured by flow dialysis (reviewed in ref *33*), is constant from about 4 to 45 °C (G. Leblanc and H.R.K., unpublished information).

Efflux. Efflux of lactose down a concentration gradient occurs in symport with H^+. When efflux from RSO vesicle containing wild-type permease is measured between 14 and 19 °C, the Arrhenius plot also exhibits a discontinuity at about 18 °C (Figure 4). Furthermore, the ratio of the E_a values observed below and above the discontinuity is about 7.1, very close to that observed for active transport. Thus, two modes of lactose translocation that involve coupled translocation of sugar with H^+ (i.e., symport) exhibit discontinuities at essentially the same temperature and similar E_a ratios below and above the transition.

Equilibrium Exchange. As discussed above with regard to the kinetic scheme shown in Figure 2, equilibrium exchange occurs without H^+ translocation and involves only steps 2 to 4. The protonated permease binds substrate on one side of the membrane, undergoes a conformational change corresponding to translocation of the ternary complex to the other side of the membrane, followed by exchange of bound substrate without loss of H^+ and reversal of the cycle. Although equilibrium exchange catalyzed by wild-type permease also exhibits a discontinuity at about 18 °C, the ratio of E_a values below and above the discontinuity is markedly reduced to a value of about 2.5 (Figure 5).

E325A permease is completely unable to catalyze active lactose transport, but permease with neutral replacements at this position binds ligand and catalyzes equilibrium exchange and counterflow at least as well as wild-type permease (*25*, *26*, *34*). Remarkably, equilibrium exchange catalyzed by the E325A mutant exhibits a completely linear Arrhenius function with an E_a of about 9.3 kcal/mol (38.9 kJ/mol) (Figure 6).

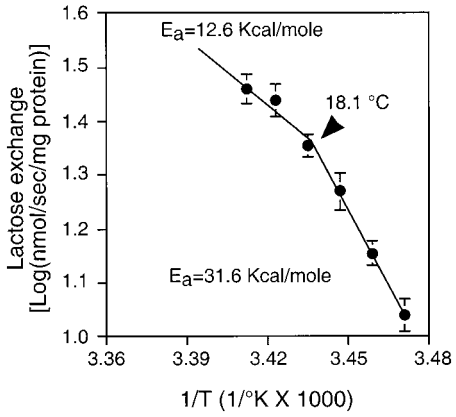

FIGURE 5: Arrhenius plot of equilibrium lactose exchange by RSO membrane vesicles containing wild-type lac permease. RSO vesicles were equilibrated with 10 mM [1-^{14}C]lactose and assayed after dilution into equilibration buffer with 10 mM nonradioactive lactose at given temperatures, as described in Experimental Procedures. Initial rates of [1-^{14}C]lactose efflux were estimated from the initial linear phase of transport (i.e., within 5 s). The results shown are the average of at least four independent experiments, and the bars represent the SEM. E_a values were calculated from the slopes shown by using the Arrhenius equation (see ref *8*). The arrowhead depicts the temperature at which the discontinuity occurs.

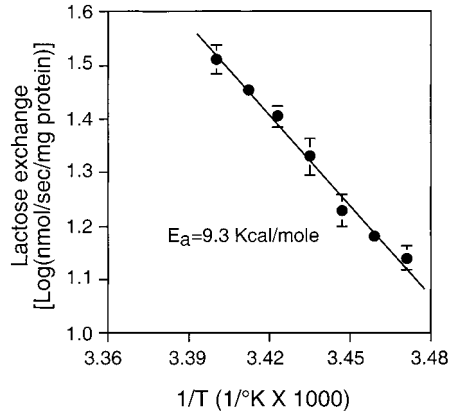

FIGURE 6: Arrhenius plot of equilibrium lactose exchange by RSO membrane vesicles containing E325A permease. RSO vesicles were equilibrated with 10 mM [1-^{14}C]lactose and assayed by dilution into equilibration buffer with 10 mM nonradioactive lactose at given temperatures, as described in Experimental Procedures. Initial rates of [1-^{14}C]lactose efflux were estimated from the initial linear phase of transport (i.e., within 5 s). The results shown are the average of at least four independent experiments, and the bars represent the SEM. E_a values were calculated from the slopes shown by using the Arrhenius equation (see ref *8*).

DISCUSSION

Membrane proteins that catalyze active transport are generally sensitive to lipid composition and dynamics, and conversion of the fatty acyl side chains of the membrane phospholipids from an ordered, gel-like state below the phase transition to a disordered, more liquid-like state above the phase transition often lowers the E_a, producing a break in the Arrhenius plot (*8*, *35*). However, the mechanism by which the lipid phase transition produces this effect is unclear, although it has been postulated to alter the conformational change that results in translocation of substrate across the membrane (see ref *8*).

The data presented here corroborate previous evidence (*5*, *6*, *11*, *12*) demonstrating that lactose accumulation driven by the proton electrochemical gradient is acutely sensitive to the lipid phase transition, exhibiting a 7−8-fold decrease in E_a above 18 °C, the temperature at which the phase transitions occurs in the membrane of wild-type *E. coli*. Similarly, lactose efflux down a concentration gradient, a reaction that also involves H^+ symport, also exhibits a sharp transition in activity that correlates with the lipid phase transition with essentially the same ratio of E_a values. In contrast, the effect of the lipid phase transition on equilibrium exchange, a reaction that does not involve proton translocation, is much less marked with wild-type permease, exhibiting only a 2−3-fold decrease in E_a above 18 °C. More importantly, mutant E325A which is specifically defective in all reactions that involve H^+ symport but catalyzes equilibrium exchange and counterflow as well as wild-type permease (*25*, *26*, *36*) exhibits a completely linear Arrhenius plot with respect to equilibrium exchange and an E_a of 9.3 kcal/mol that approximates the E_a values observed for active transport and efflux above the phase transition. Thus, the conformational change in the permease that corresponds to the translocation step in the overall mechanism (Figure 2, step 3) appears to be completely unaffected by the lipid phase transition. Given this conclusion, it is reasonable to suggest that the primary effect of the phase transition is on the coupling between lactose and H^+ translocation.

Recent studies (*34*) in which ligand binding was measured as a function of pH in wild-type permease and mutants in Glu325, Arg302, His322, and Glu269 have led to a proposed mechanism for lactose/H^+ symport that is consistent with the kinetic scheme described. In the ground state, the permease is protonated, the H^+ is shared between His322 and Glu269, while Glu325 is charge-paired with Arg302, and substrate is bound with high affinity at the interface between helices IV (Glu126) and V (Arg144 and Cys148) which is accessible from the outside surface of the membrane. Substrate binding induces a conformational change that leads to transfer of the H^+ from His322/Glu269 to Glu325 and reorientation of the binding site to the inner surface with a decrease in affinity and dissociation of substrate. Glu325 is then deprotonated on the inside due to re-juxtaposition with Arg302. The His322/Glu269 complex is then reprotonated from the outside surface to reinitiate the cycle.

Under conditions of exchange or counterflow where substrate is saturating on both sides of the membrane, Glu325 does not deprotonate, and the permease oscillates back and forth between inwardly and outwardly facing conformations, binding and releasing substrate on alternative sides of the membrane. In this regard, it is noteworthy that D_2O (*37*) or monoclonal antibody 4B1 (*38*, *39*) which binds to an epitope in the periplasmic loop between helices VII and VIII (*40*) mimicks the phenotype of neutral replacements for Glu325. In addition, site-directed fluorescence quenching studies with bromo-dodecylmaltopyranoside (*41*) indicate that the face of helix X with Glu325 becomes more accessible to a hydrophobic environment in the presence of ligand. Taking the findings as a whole, it seems reasonable to suggest that the primary effect of the lipid phase transition is related to an effect on Glu325. During reactions that involve H^+ symport when Glu325 is alternatively exposed to the low dielectric of the membrane as the protonated carboxylic acid or re-juxtapositioning with Arg302 as the unprotonated carboxylate, respectively, a higher activation energy might

be required when the immediate environment is in a gel-like state. Alternatively, during exchange, Glu325 remains protonated, continuously accessible to the low dielectric of the membrane, and the exchange reaction is insensitive to the lipid phase transition. It is also possible that during exchange, a H^+ moves back and forth between Glu269/His322 and His322/Glu325 which would account for the small but discernible break in the Arrhenius plot with wild-type permease.

Finally, it is noteworthy that in addition to lac permease, other symporters, such as the β-glucoside/H^+ symporter of *E. coli* for example (*6*, *12*), also respond similarly to the lipid phase transition with respect to uphill accumulation. Moreover, ATP synthesis catalyzed by the membrane-bound *E. coli* F_1F_0 ATP synthase complex (*42*) exhibits a discontinuity at around 19 °C, while the soluble F_1 portion exhibits a linear Arrhenius plot from 5 to 45 °C with respect to ATP hydrolysis. The difference in behavior is likely due to the effect of the lipid phase transition on the H^+ translocating function of the F_0 portion of the complex (see ref *43*). In contrast, vectorial phosphorylation of glucose in *E. coli* is catalyzed by the phosphoenolpyruvate:carbohydrate phosphotransferase system (*44*, *45*), while glucose transport in human erythrocytes (*35*) or fat cells (*46*) occurs by facilitated diffusion (i.e., uniport). In marked contrast to those systems that catalyze symport, glucose transport in *E. coli* (*47*) erythrocytes (*35*) and fat cells (*46*) exhibits linear Arrhenius plots over the temperature range where the lipid phase transition occurs.

ACKNOWLEDGMENT

We acknowledge Miklós Sahin-Tóth for valuable advice and providing the E325A mutant, as well as Christopher D. Wolin for helpful discussions.

REFERENCES

1. Engelman, D. M. (1971) *J. Mol. Biol. 58*, 153−165.
2. McElhaney, R. N. (1982) *Chem. Phys. Lipids 30*, 229−259.
3. Overath, P., Brenner, M., Gulik-Krzywicki, T., Shechter, E., and Letellier, L. (1975) *Biochim. Biophys. Acta 389*, 358−369.
4. Engelman, D. M. (1970) *J. Mol. Biol. 47*, 115−117.
5. Schairer, H. U., and Overath, P. (1969) *Biochemistry 16*, 1283−1289.
6. Wilson, G., and Fox, C. F. (1971) *J. Mol. Biol. 55*, 49−60.
7. Overath, P., and Trauble, H. (1973) *Biochemistry 12*, 2625−2634.
8. McElhaney, R. N. (1982) *Curr. Top. Membr. Transp. 17*, 317−370.
9. Wilson, G., Rose, S. P., and Fox, C. F. (1970) *Biochem. Biophys. Res. Commun. 38*, 617−623.
10. Linden, C. D., and Fox, C. F. (1975) *Acc. Chem. Res. 8*, 321−327.
11. Kaback, H. R., and Barnes, E. M., Jr. (1971) *J. Biol. Chem. 246*, 5523−5531.
12. Thilo, L., Trauble, H., and Overath, P. (1977) *Biochemistry 16*, 1283−1290.
13. Kaback, H. R. (1976) *J. Cell. Physiol. 89*, 575−593.
14. Kaback, H. R. (1983) *J. Membr. Biol. 76*, 95−112.
15. Poolman, B., and Konings, W. N. (1993) *Biochim. Biophys. Acta 1183*, 5−39.
16. Varela, M. F., and Wilson, T. H. (1996) *Biochim. Biophys. Acta 1276*, 21−34.
17. Viitanen, P., Newman, M. J., Foster, D. L., Wilson, T. H., and Kaback, H. R. (1986) *Methods Enzymol. 125*, 429−452.
18. Sahin-Tóth, M., Lawrence, M. C., and Kaback, H. R. (1994) *Proc. Natl. Acad. Sci. USA 91*, 5421−5425.
19. Kaback, H. R. (1996) in *Handbook of Biological Physics: Transport Processes in Eukaryotic and Prokaryotic Organisms* (Konings, W. N., Kaback, H. R., and Lolkema, J. S., Eds.) pp 203−227, Elsevier, Amsterdam.
20. Kaback, H. R., and Wu, J. (1997) *Q. Rev. Biophys. 30*, 333−364.
21. Kaback, H. R., and Wu, J. (1999) *Acc. Chem. Res. 32*, 805−813.
22. Frillingos, S., Sahin-Tóth, M., Wu, J., and Kaback, H. R. (1998) *FASEB J. 12*, 1281−1299.
23. Kaczorowski, G. J., Robertson, D. E., and Kaback, H. R. (1979) *Biochemistry 18*, 3697−3704.
24. Kaczorowski, G. J., and Kaback, H. R. (1979) *Biochemistry 18*, 3691−3697.
25. Carrasco, N., Puttner, I. B., Antes, L. M., Lee, J. A., Larigan, J. D., Lolkema, J. S., Roepe, P. D., and Kaback, H. R. (1989) *Biochemistry 28*, 2533−2539.
26. Carrasco, N., Antes, L. M., Poonian, M. S., and Kaback, H. R. (1986) *Biochemistry 25*, 4486−4488.
27. He, M., and Kaback, H. R. (1997) *Biochemistry 36*, 13688−13692.
28. Teather, R. M., Bramhall, J., Riede, I., Wright, J. K., Furst, M., Aichele, G., Wilhelm, V., and Overath, P. (1980) *Eur. J. Biochem. 108*, 223−231.
29. Kaback, H. R. (1971) *Methods in Enzymol. XXII*, 99−120.
30. Short, S. A., Kaback, H. R., and Kohn, L. D. (1975) *J. Biol. Chem. 250*, 4291−4296.
31. Konings, W. N., Barnes, E. M., Jr., and Kaback, H. R. (1971) *J. Biol. Chem. 246*, 5857−5861.
32. Kaback, H. R. (1974) *Methods Enzymol. 31*, 698−709.
33. Ramos, S., Schuldiner, S., and Kaback, H. R. (1979) *Methods Enzymol. 55*, 680−8.
34. Sahin-Tóth, M., Karlin, A., and Kaback, H. R. (2000) *Proc. Natl. Acad. Sci. U.S.A. 97*, 10729−10732.
35. Carruthers, A., and Melchior, D. L. (1988) *Annu. Rev. Physiol. 50*, 257−271.
36. Kaback, H. R. (1987) *Biochemistry 26*, 2071−6.
37. Viitanen, P., Garcia, M. L., Foster, D. L., Kaczorowski, G. J., and Kaback, H. R. (1983) *Biochemistry 22*, 2531−6.
38. Carrasco, N., Tahara, S. M., Patel, L., Goldkorn, T., and Kaback, H. R. (1982) *Proc. Natl. Acad. Sci. USA 79*, 6894−6898.
39. Carrasco, N., Viitanen, P., Herzlinger, D., and Kaback, H. R. (1984) *Biochemistry 23*, 3681−7.
40. Sun, J., Wu, J., Carrasco, N., and Kaback, H. R. (1996) *Biochemistry 35*, 990−8.
41. Wang, Q., Matsushita, K., de Foresta, B., LeMaire, M., and Kaback, H. R. (1997) *Biochemistry 36*, 14120−14127.
42. Al-Shawi, M. K., Ketchum, C. J., and Nakamoto, R. K. (1997) *J. Biol. Chem. 272*, 2300−2306.
43. Rastogi, V. K., and Girvin, M. E. (1999) *Nature 402*, 263−268.
44. Kaback, H. R. (1968) *J. Biol. Chem. 243*, 3711−3724.
45. Postma, P. W., Lengeler, J. W., and Jacobson, G. R. (1996) in *Escherichia coli and Salmonella typhimurium*: Cellular and Molecular Biology (Neidhardt, F. C., Ed.) pp 1149−1174, American Society of Microbiology, Washington, DC.
46. Ezaki, O., and Kono, T. (1982) *J. Biol. Chem. 257*, 14306−14310.
47. Rottem, S., Cirillo, V. P., Kruyff, B. d., Shinitzky, M., and Razin, S. (1973) *Biochim. Biophys. Acta 323*, 509−519.

BI001947G